Liquid-Liquid Phase Separation for Analyte Enrichment in Coacervates for Ultra-Sensitive Biosensing

Chaofeng Cen[1], Xudong Ma[2], Xi Lu[1], Hui Zhou[1], Yinliang Lin[3], Si Meng[1], Wenwen Chen[1], Zhou Liu[4], Cheng Qi[2,], Tiantian Kong[1,5,*]*

[1] Department of Biomedical Engineering, School of Medicine, Shenzhen University, Shenzhen, Guangdong 518000, China
[2] Guangdong Provincial Key Laboratory of Micro/Nano Optomechatronics Engineering, College of Mechatronics and Control Engineering, Shenzhen University, Shenzhen, Guangdong 518000, China
[3] College of Chemistry and Chemical Engineering, Southwest Petroleum University, Chengdu, 610500, PR China
[4] College of Chemistry and Environmental Engineering, Shenzhen University, Shenzhen, Guangdong 518000, China
[5] Department of Urology, Shenzhen Institute of Translational Medicine, The First Affiliated Hospital of Shenzhen University, Shenzhen Second People's Hospital, Shenzhen, Guangdong 518037, China

*Corresponding authors.
E-mail addresses: cqi@szu.edu.cn (C. Qi); ttkong@szu.edu.cn (T. Kong)

Keywords: coacervate, liquid-liquid phase separation (LLPS), aqueous two-phase system (ATPS), DNA, biosensing, enrichment

Abstract

Efficient isolation and concentration of biomarkers are foundational for rapid diagnostics. Traditional methods, often reliant on solid surfaces, necessitate complex and labor-intensive procedures. Liquid-liquid phase separation (LLPS) systems have emerged as promising due to their ability to extract biomolecules via the partitioning effect. Inspired by the biomolecular compartmentalization observed in cellular organelles, we prepared coacervates via associative LLPS for concentrating a diverse range of biomolecules, significantly enhancing sensitivity and lowering detection limits of biomolecules by condensing biomolecules in compartments. We demonstrated that under optimal conditions these coacervates achieved an enrichment factor of up to 22.8 for DNA, surpassing the efficiency of aqueous two-phase systems (ATPS) formed by segregative LLPS. The results significantly enhanced sensitivity for DNA and ATP

detections. By means of fluorescence microscopy, microplate readers, and flow cytometry, we established that the coacervate-based system were approximately 21 times more effective in reducing the limit of detection (LOD) for DNA compared to ATPS. The superior performance of coacervate-based system is attributed to non-covalent interactions between DNA and molecules within coacervates, enabling ultra-sensitive quantification without the need for complex instrumentation or signal amplification. By creating distinct compartments for biomolecule condensation, our approach not only simplifies the detection process but also significantly lowers detection thresholds, paving the way for more accessible and rapid diagnostic methods.

Introduction

Rapid and point-of-care diagnostics are paramount in timely healthcare interventions.[1] Central to their effectiveness often hinges on the ability of efficient sensing of target biomolecules.[2] Concentrating analytes or biomarkers can accelerate reactions, enhance sensitivity, and establish lower detection thresholds. Typical strategies encompass target amplification, signal augmentation, and local concentration of biomolecules. For instance, Polymerase Chain Reaction (PCR) amplifies the target DNAs to optimize detection;[3-4] while Enzyme-Linked Immunosorbent Assay (ELISA) harnesses antibody-antigen interactions for specific targeting and utilizes enzymatic reactions to amplify the signal.[5-6] To locally concentrate targets for detection, solid surfaces like magnetic beads or hydrogel particles are employed to anchor and locally concentrate targets, which can be subsequently isolated using techniques such as external electromagnetic fields[7] or microfluidics[5]. However, these methods often require intricate instrumentations and labor-intensive washing steps, attenuating their practicability for real-time diagnostics.

Single-step enrichment techniques have emerged in the pursuit of efficient biosensing. Conventional DNA extraction methods, for instance, rely on potentially hazardous chemicals like phenol-chloroform and are time-consuming.[8-9] In contrast, Aqueous Two-Phase Systems (ATPS) have arisen as a straightforward, safe, biocompatible and wash-free option for biomolecule isolation.[10-13] Owing to

segregative phase separation, ATPS forms when two water-soluble polymers, or a polymer and a salt are mixed at sufficiently high concentrations.[14-15] ATPS allows biomolecules to be partitioned into one of their phases, based on relative affinity. This segregation increases local concentrations, thus bolstering detection sensitivity.[16-19] It was reported that DNA could be enriched around seven times in ATPS and its detection of limit could be improved by 3.6-fold.[19]

In living cells, a large variety of membraneless organelles are biomolecular condensates providing crowded compartments for biomolecules to fulfill their biochemical functions.[20-23] Formation of these biomolecular condensates (also known as coacervate) is owing to another kind of LLPS, i.e., associative LLPS, and they have been successfully reconstituted *in vitro*.[24] Coacervates exhibit a strong capacity of concentrating a wide range of biomolecules or substances such as living bacteria, proteins and nucleic acids.[25-27] Inspired by this feature, we seek to investigate its potential applicability for biomolecule detection, thereby improving biosensing performance.

In this study, we have systematically investigated the use of coacervate-based system for efficient concentration of vital biomolecules, focusing on nucleic acids and ATP, to enhance biosensor sensitivity. By employing the coacervate formed by polydiallyldimethyl ammonium (PDDA) and adenosine triphosphate (ATP) as a model of example, we systematically investigated and optimize the enrichment factor of DNA within the coacervate. As large as 22.8 enrichment factor can be reached, which is considerably more pronounced than that in ATPS, thus leading to a remarkable boost in detection sensitivity. We also demonstrated the establishment of a linear correlation between the detected DNA concentration and their fluorescence intensity, as well as high specificity for the target biomolecules, both highlighting the precision and reliability of the coacervate approach. By leveraging various analytical methods, including fluorescence microscopy, microplate reading, and flow cytometry, we determined that the coacervate-based system were about 21 times more effective in lowering the limit of detection (LOD) for DNA, compared to ATPS. This enhanced performance can be attributed to the non-covalent interactions between DNA and

PDDA molecules, facilitating ultra-sensitive detection without the necessity of complex instrumentation or signal amplification. Our results highlighted the significant advantages of coacervate-based biosensors, especially their greater sensitivity and lower detection limits. To the best of authors' knowledge, this study is the first to propose a coacervate-based system for biomolecule detection. Our work may pave the way for the development of more efficient, cost-effective, and accessible diagnostic methods. These methods, tailored for easy implementation in low-resource settings, have the potential to meet critical global healthcare needs effectively.

Results and Discussion

To enrich and segregate target biomolecules within coacervates, we utilized DNA molecules as a model of example to investigate their enrichment. To facilitate visualization and quantification, we employed DNA molecules tagged with anthocyanin fluorescent dye (Cy5), and chose PDDA and ATP to form coacervate for enriching Cy5-DNA molecules. ATP molecules containing three phosphate groups are negatively charged, and thus they can complex with positively charged PDDA molecules to form coacervates, as schematically described in **Figure 1a(i)**. We prepared the sample by mixing PDDA, ATP and Cy5-DNA, and observed micrometer-sized coacervate droplets that emitted red fluorescence under the confocal microscope (Figure 1a(ii)). It indicated that DNA molecules were well enriched in the coacervate phase.

To analyze the DNA enrichment within the coacervate phase, we allowed the mixed sample to stand undisturbed for 30 minutes until it separated into the upper dilute and lower condensed coacervate phases within a centrifuge tube. We then collected the coacervate phase from the bottom of the tube and pipetted one drop of it onto the glass slide for observation under the confocal microscope. At different given concentrations of DNA, the corresponding fluorescent intensities (or gray values) could be measured. Therefore, a quantitative relationship between the concentration of DNA and fluorescent intensity was established for subsequent data analysis. The whole process described above was schematically depicted in Figure 1b. To quantify the DNA

enrichment within the coacervate phase, we defined a nondimensional enrichment factor which denoted the concentration ratio of DNA in the coacervate phase to the diluted phase (detailed calculation of the enrichment factor was provided in Experimental section).

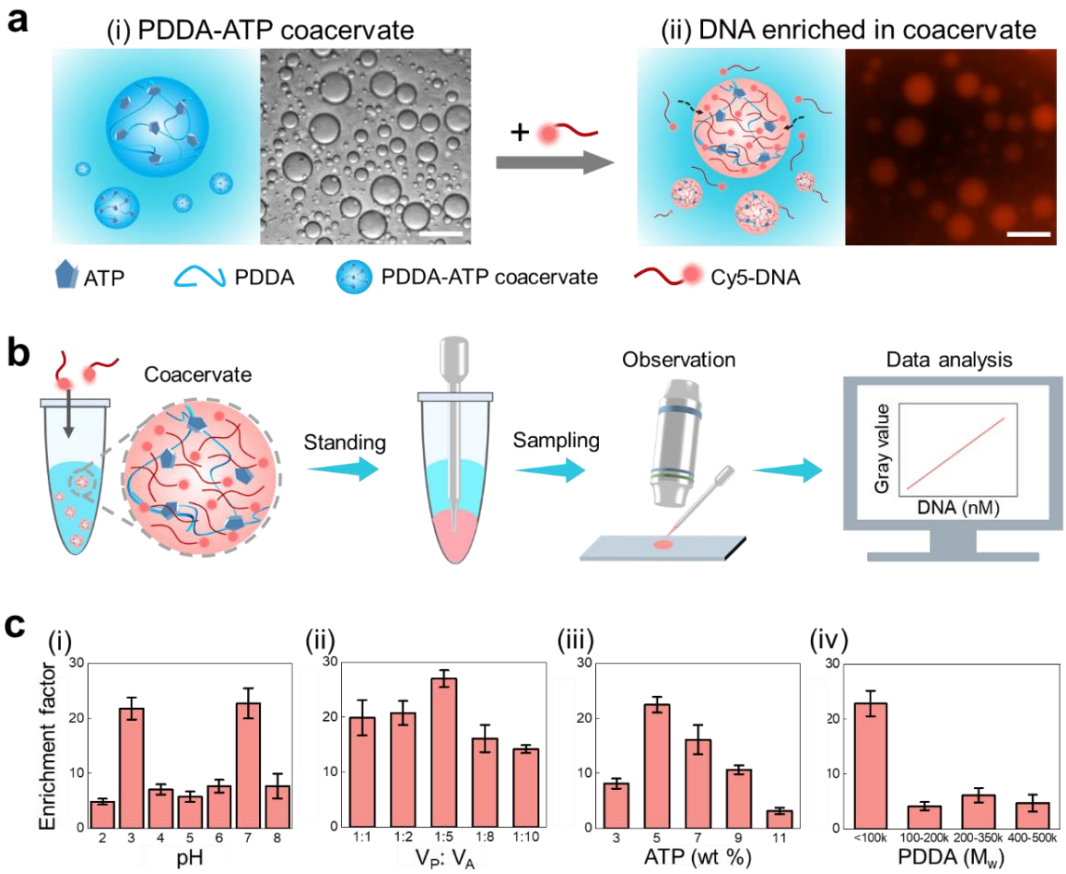

Figure 1. DNA enrichment in PDDA-ATP coacervate phases under different conditions. a. Schematic and optical microscopy images of (i) PDDA-ATP coacervate droplets and (ii) DNA-enriched PDDA-ATP coacervate droplets. The sample contained 2.5 wt % PDDA, 2.5 wt % ATP and 1 μM Cy5-DNA (red fluorescence). Scale bars are 50 μm. b. Schematic diagrams describing the whole process for target DNA detection. c. Effects of (i) pH values, (ii) volume ratios of PDDA to ATP solutions (V_P: V_A), (iii) ATP concentrations, and (iv) PDDA molecular weights. The compositions of tested samples were given in Experimental section and their fluorescent images were provided in Figure S3-S6. Fluorescent images were obtained at the same settings of the confocal microscope (analog gain = 11.4x).

Associative LLPS of PDDA and ATP is largely affected by polymer molecular weight of PDDA, volume ratio of PDDA to ATP solutions (V_P: V_A), ATP concentration (C_{ATP}), and pH.[28-29] We systematically investigated the effects of these factors on the enrichment factor in Figure 1c. By adjusting the pH of the sample, it was observed that

within the pH value ranging from 2 to 8, DNA consistently showed a significant enrichment in the coacervate phase, between 4.8 and 22.7, as illustrated in Figure 1c(i). Notably, the enrichment factors reached 21.8 and 22.7 at pH = 3 and pH = 7, respectively. However, at extreme pH values, specifically below 1.5 or above 12, associate LLPS of PDDA and ATP did not occur and hence DNA molecules were uniformly distributed in the mixed sample. Another influential factor is the molecular weight of PDDA. The results in Figure 1c(ii) suggested that coacervates composed of PDDA with lower molecular weight (< 100 kDa) demonstrated superior enrichment, reaching up to 22.8. In contrast, coacervates formed by higher molecular weights (100 kDa ~ 500 kDa) had the enrichment factor ranging from 4.1 to 6.1. The enrichment factor was not so sensitive to V_P: V_A and the ATP concentration as to pH and the molecular weight of PDDA, as evidenced by Figures 1c(iii) and 1c(iv). By the systematical parametric analysis, we can determine the optimal condition for DNA enrichment. Therefore, in the following experiments, we prepared the coacervate samples at the condition of pH = 7, V_P: V_A = 1:1, $C_{ATP} = 5$ wt % and molecular weight < 100 kDa (for PDDA).

The strong enrichment of DNA within the coacervate phase effectively amplifies the local concentration of DNA. To identify target DNA sequences within the coacervate phase, we employed molecular beacons (MB) as fluorescent reporters. MB is a single-stranded DNA fragment and exhibits a similar enrichment effect within the coacervate phase. MB is engineered with a fluorophore on one end and a quencher (black hole) on the other. Without the presence of the target DNA, MB remains in a hairpin structure, emitting only a faint fluorescence. However, upon specific binding to the target DNA, the beacon's structure unfolds, revealing a pronounced fluorescence signal, as shown in **Figure 2a**.

We captured fluorescent images of different concentrations of target DNA as well as a negative control where a blank sample only contained MB in Figure 2b. As the DNA concentration increased, a proportional increasing brightness was displayed. Their corresponding quantitative data were shown in Figure 2c. The relationship between the target DNA concentration and the fluorescence intensity demonstrated a

well linear fitting with a high correlation coefficient $R^2 = 0.9967$. Therefore, the fluorescence intensity can be used to accurately evaluate the concentration of the target DNA.

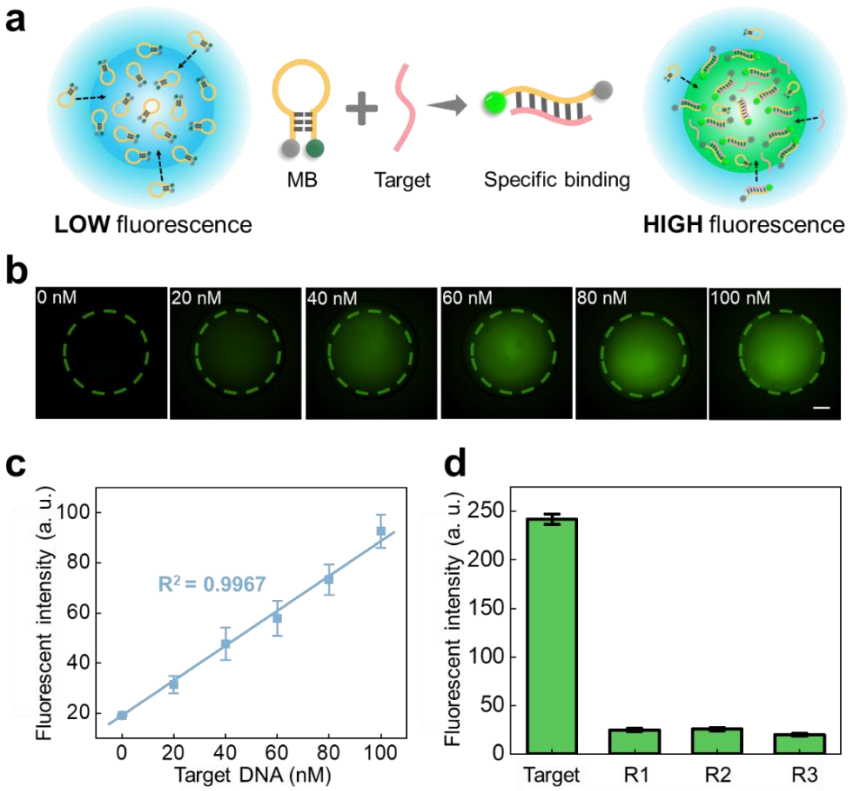

Figure 2. Target DNA detection in PDDA-ATP coacervate system. a. Schematic diagram of DNA detection mechanism. b. Confocal fluorescent images of the samples containing different concentrations of target DNA. The coacervate was prepared by mixing 2.5 wt % PDDA (M_w < 100 kDa) and 2.5 wt % ATP at pH = 7. Scale bar is 500 μm. c. Measured fluorescent intensities as a function of different concentrations of the target DNA, where they are quite linearly related with the coefficient of determination $R^2 = 0.9967$. d. A plot of fluorescence intensities showing the specificity of the target detection in the coacervate-base system. R1, R2, and R3 are random DNA sequences with the same number of bases as the target DNA sequence.Fluorescent images were obtained at the same settings of the confocal microscope (analog gain = 7.6x).

To study reliability of our approach for detecting target DNA molecules, we prepared three additional DNA molecules with random sequences R1, R2 and R3 (**Table 1**), which had the same base number as the target DNA. We compared their fluorescence intensities in the coacervate phase with that of the target DNA in Figure 2d, where no obvious fluorescence could be observed for the random DNA sequences R1, R2 and R3. Even when the concentration of the random DNA sequences was

increased to five times as large as that of the target DNA, the fluorescence was still hardly to be detected. This indicated that MB did not bind with these random DNA sequences. Thus, using MB to detect the target in the coacervates is highly specific.

ATP is one of the most pivotal biomolecules in living organisms and its detection is important for monitoring cellular physiology and metabolism. We further investigated the effectiveness and robustness of the coacervate system for sensing and detecting ATP. To this end, we engineered PDDA-ATP aptamer coacervates (**Figure 3a(i)**). ATP aptamer is a single stranded DNA (ssDNA) that is negatively charged and hence can be electrostatically complexed with positively charged PDDA molecules. In this coacervate system, thioflavin T (ThT) was also added. It could be concentrated in the preformed PDDA-ATP aptamer coacervates and intercalated into ATP aptamers to emit strong fluorescence signals (Figure 3a(ii)).

The combination of ThT and ATP aptamer in the coacervate gives strong fluorescent intensity, however, the intensity will be weakened by the presence of ATP. ATP will bind strongly with ATP aptamers, resulting in the release of ThT from ATP aptamers (Figure 3b). Therefore, upon adding ATP into the coacervate system, the fluorescent intensity will be decreased accordingly (Figure 3c). The fluorescent intensity as a function of ATP concentration was plotted in Figure 3d. The results exhibited a favorable linear relationship with a high correlation coefficient ($R^2 = 0.9930$). The limit of detection (LOD) of ATP detection was calculated to be 0.029 μM. We also verified the specificity of ATP detection by introducing CTP and GTP while keeping other parameters consistent. No significant reduction in detected fluorescent intensity was noted, as shown in Figure 3e, signifying the specificity of ATP detection by the proposed coacervate system.

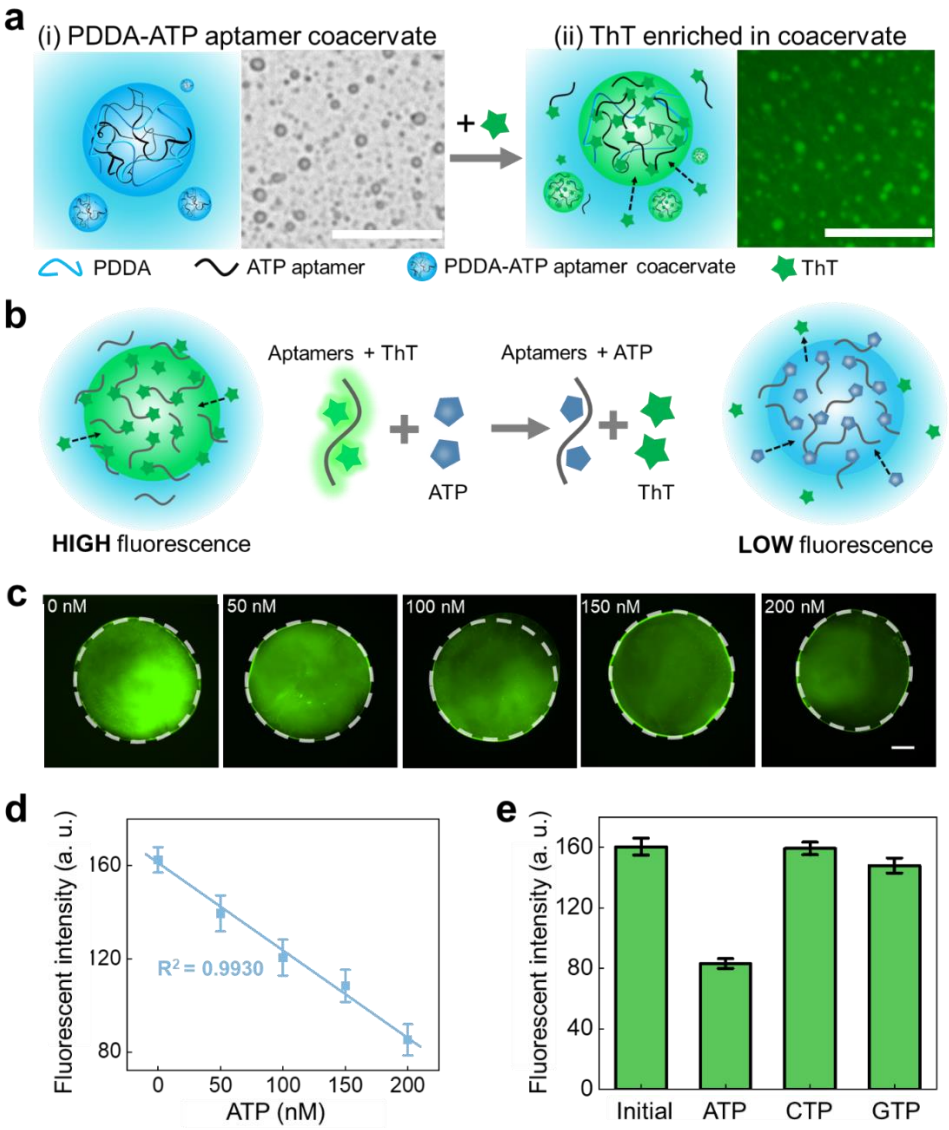

Figure 3. ATP detection in PDDA-ATP aptamers coacervate droplets. a. Schematic and optical microscopy images of (i) PDDA-ATP aptamer coacervate droplets and (ii) ThT enriched PDDA-ATP aptamer coacervate droplets. Inside the coacervate droplets, ThT was intercalated into ATP aptamers to emit strong fluorescence signals. b. Schematic diagram of ATP detection mechanism. c. Confocal fluorescent images of the samples containing different concentrations of ATP. d. Standard line depicting the relationship between the ATP concentration and the fluorescence intensity, with a correlation coefficient $R^2 = 0.9930$. e. A plot of fluorescence intensities showing the specificity of the target detection by the coacervate system. The sample was prepared by adding 0.5 wt % PDDA (M_w < 100 kDa), 50 μM ATP aptamer and/or 2 μM ThT into a tube. Scale bars are 50 μm. Fluorescent images were obtained at the same settings of the confocal microscope (analog gain = 7.6x).

Compartmentation formed owing to LLPS is able to partition and concentrate biomolecules spontaneously. For instance, associative LLPS within living cells gives

rise to the formation of biomolecular condensates, which can enrich proteins and RNA and accelerate their reactions.[30-31] ATPS resulting from non-associative LLPS has been utilized to partition DNA probes for improving detection efficiency and lowering detection limits.[19] In a typical ATPS, dextran and PEG mixture with sufficiently high concentrations will phase-separate into dextran-rich and PEG-rich phases.[14, 32-33] It was previously proved that the dextran-rich phase could enrich DNA molecules and achieve sensitive sensing of target DNA.[19] To investigate the capabilities of both types of LLPS in enhancing the performance of target DNA detection, we examined both the typical associative LLPS system (PDDA-ATP coacervate) and non-associative LLPS system (PEG-dextran ATPS) by conducting comparative analyses through fluorescence microscope, microplate reader and flow cytometry (**Figure 4**).

We first compared the biosensing performance of PDDA-ATP coacervate and PEG-dextran ATPS through fluorescence microscope (Figure 4a) in detecting target DNA. We took the two samples (coacervate and dextran-rich phases) with the same volume for testing by the fluorescence microscope. Fluorescence intensity distributions across dextran-rich and coacervate droplets containing different concentrations of target DNA are displayed in Figures 4a(i) and 4a(ii), and the comparison of their average fluorescence intensities is summarized in Figure 4a(iii). It is obviously that the intensity of the coacervate is much more significant than that of the dextran-rich droplet. This indicated that the concentration of DNA was much higher in the coacervate and hence the DNA detection was more sensitive by means of coacervate-based method.

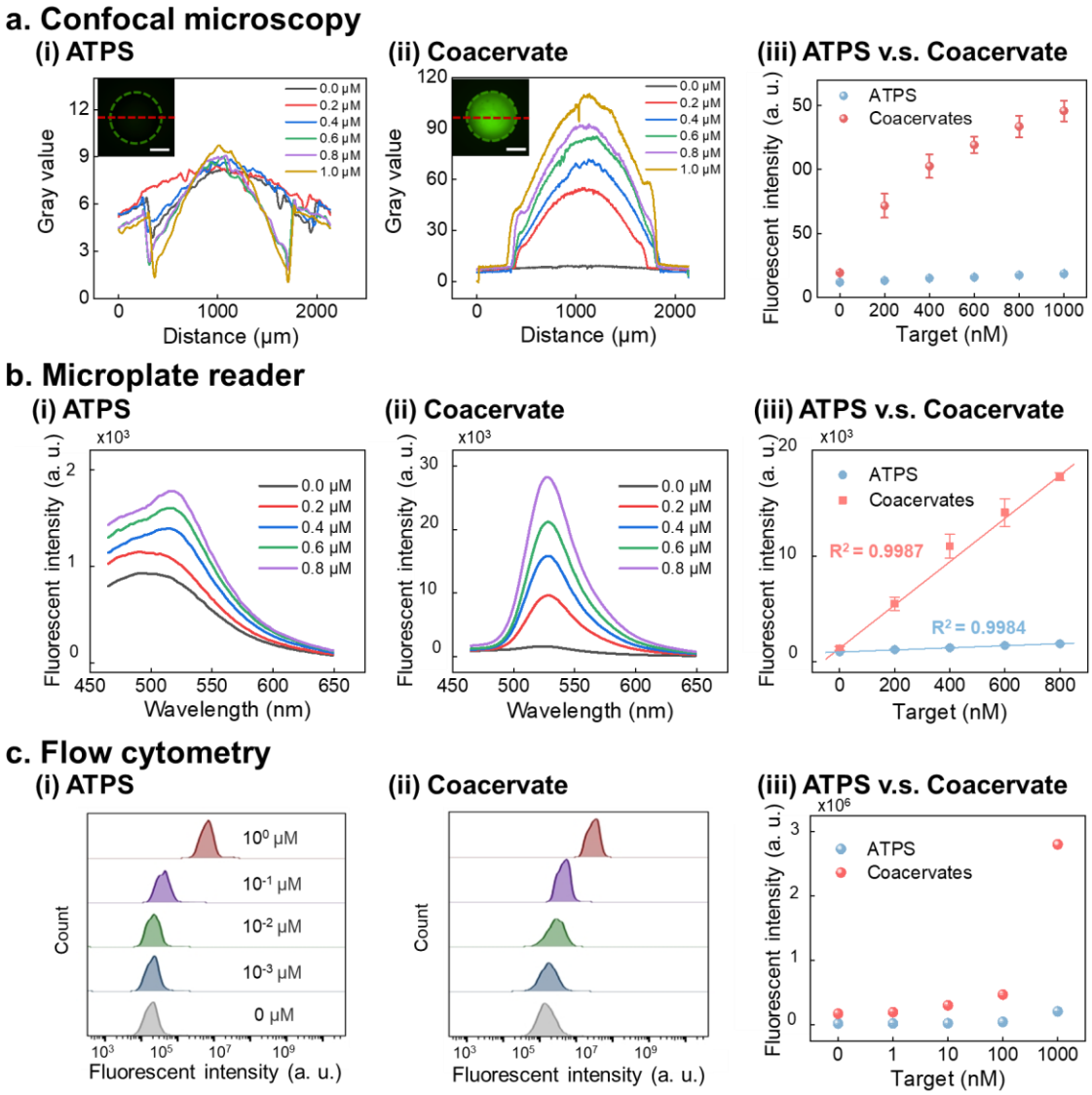

Figure 4. Comparison of DNA detection performances by PEG/dextran ATPS and PDDA-ATP coacervate system. The detection results at different concentrations of target DNA were analyzed by the apparatus of a. confocal microscope, b. microplate reader and c. flow cytometry. By mixing 8 wt % dextran and 10 wt % PEG at pH = 7, the solution was phase-separated into PEG-rich and dextran-rich phases.[19] According to Ref. [19], the target DNA could be concentrated in the dextran-rich phase. Then, the DNA-enriched dextran-rich phase was sampled for testing. The PDDA-ATP coacervate was prepared by mixing 2.5 wt % PDDA (M_w < 100 kDa), 2.5 wt % ATP, and DNA at pH = 7. In (a), the inserts were the confocal images where the 1μM target DNA was contained. Scale bars are 1 mm. Fluorescent images were obtained at the same settings of the confocal microscope (analog gain = 5.1x).

Since the fluorescent signal in the dextran-rich phase could be hardly detected by the confocal microscope (insert in Figure 4a(i)), we further used microplate reader and flow cytometry to determine its fluorescence intensity and made a comparison with that

in the coacervate phase. The results obtained by both of these two methods indicated that the coacervate system showed a better sensing performance since its fluorescent intensity was more sensitive towards the variation of DNA concentration in the coacervate phase (Figures 4b(iii) and 4c(iii)). By using the microplate reader, the fluorescent intensity varied linearly with the concentration of the target DNA molecule for both coacervate system and ATPS. Based on these lines, LOD of the coacervate system and ATPS could be determined to be 5.17×10^{-4} μM and 1.12×10^{-2} μM, respectively. It indicated that the coacervate system is roughly 21 times more effective in lowering LOD compared to the ATPS. In addition, the flow cytometry was used to make a comparison of sensing performance between coacervate system and ATPS at an individual microdroplet level (Figure 4c). As expected, the coacervate system also exhibited a better sensibility towards the concentration of the target DNA (Figure 4c(iii)).

The result in Figure 4 indicates that the coacervate-base system exhibits better performance of target DNA detection than the ATPS. It is largely attributed to stronger enrichment of DNA in the coacervate. In the PEG-dextran ATPS, DNA tended to concentrate in the bottom dextran-rich phase (**Figure 5a**, where Cy5-DNA emitted light blue under visible light) because of its hydrophilic structure due to sugar-phosphate backbone.[34] If the coacervate was added into the preformed ATPS, a three-phase system would be formed. After standing or centrifugation, the solution stratified into the top PEG-rich phase, middle dextran-rich phase and bottom coacervate phase in the tube. Then, Cy5-DNA was mostly enriched in the coacervate, instead of the dextran-rich phase (Figure 5a). This was verified by fluorescent intensities of these two phases. The concentration of DNA in the coacervate was at least one order of magnitude larger than that in the dextran-rich phase. If we emulsified the three-phase system in the tube, a core-shell architecture was form observed by the confocal microscope: the coacervate was the core and the dextran-rich phase was the shell (Figure 5b). It was clear that at a microdroplet level Cy5-DNA was also mostly enriched in the coacervate phase.

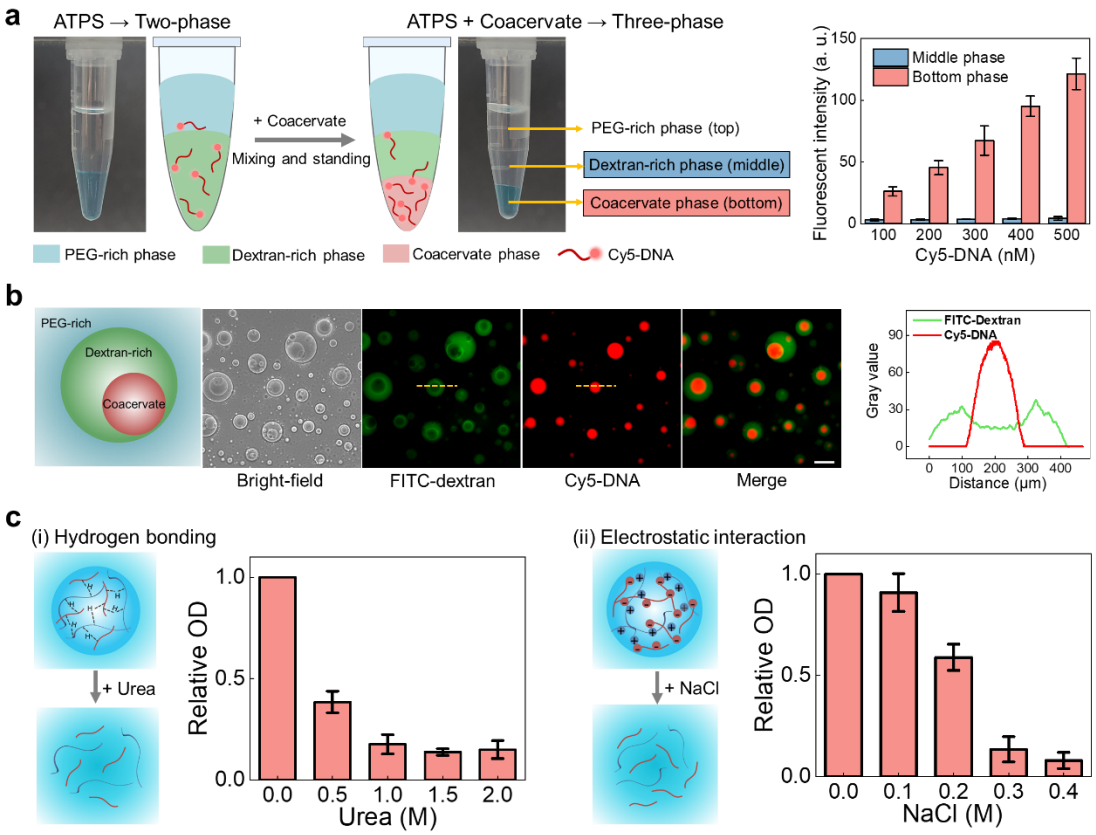

Figure 5. Intermolecular interactions between DNA and coacervate. a. Cy5-DNA was first enriched in the dextran-rich phase in the PEG-dextran ATPS (8 wt % dextran and 10 wt % PEG at pH = 7) indicated by light blue under visible light in the tube. If coacervate (5 wt % PDDA (M_w < 100 kDa) and 5 wt % ATP) was added into the ATPS solution, an immiscible triphasic system was formed: PEG-rich, dextran-rich and coacervate located at the top, middle and bottom of the tube, respectively. In this three-phase system, Cy5-DNA was enriched in the bottom phase indicated by light blue under visible light in the tube. The results of intensity of Cy5-DNA (red fluorescence) at different concentrations were measured by the confocal microscope. b. The microscopic morphology of the three-phase system, where bight-field and fluorescent images were given. Gray values were collected across the yellow dashed line in the images of FITC-dextran and Cy5-DNA. Scale bars are 100 μm. c. Schematic diagram showing additives that can disrupt different intermolecular interactions (NaCl, electrostatic interaction; and urea, hydrogen bonding), and relative optical density (OD) at 400 nm showing a decrease in value by the titration of different concentrations of additives on PDDA-DNA coacervate (0.5 wt %PDDA and 50 μM target DNA). Fluorescent images were obtained at the same settings of the confocal microscope (analog gain = 7.6x).

DNA molecules have strong intermolecular interaction with PDDA molecules as they have been reported to undergo associate LLPS and form coacervate.[35-38] To investigate the role of their interactions responsible for LLPS, we performed coacervate dissolution assay using NaCl and urea to disrupt electrostatic interaction and hydrogen-

bonding, respectively (Figure 5c).[39] The titration of additives (NaCl or urea) into PDDA-DNA coacervate solutions resulted in distinct decrease of relative optical density (OD) of the solution. It indicated that both electrostatic effect and hydrogen-bonding played an important role in intermolecular interaction between DNA and PDDA molecules. When 0.5 M urea was added into the coacervate solution, there was a remarkable decrease in relative OD (> 60%). For the disruption by NaCl, the most significant decrease in relative OD occurred when the NaCl concentration was about 0.2 ~ 0.3 M. It seems that the combination between DNA and PDDA molecules was relatively more relying on hydrogen bonding.

Conclusion

To addresses the pressing need for rapid and efficient biomolecule isolation in point-of-care diagnostics, we innovatively employed coacervate-based LLPS to concentrate biomolecules, markedly enhancing biosensor sensitivity and specificity for nucleic acid and ATP detection. By using PDDA-ATP coacervates as a model system, we achieved a significant enrichment of nucleic acids in the coacervate phase, with an enrichment factor ranging between 4.8 and 22.7, depending on the pH and molecular weight of PDDA. This enrichment is significantly superior to that achieved by segregative LLPS, aqueous two-phase systems (ATPS), leading to more sensitive biomolecule detection. Our results revealed a linear correlation (R^2=0.9967) between DNA concentration and fluorescence intensity within coacervate droplets, allowing precise DNA quantification. Moreover, the coacervate droplets exhibited high specificity for the target DNA, binding negligibly with random DNA sequences, a key feature for accurate target detection. In ATP detection, PDDA-ATP aptamer coacervates achieved an impressively low limit of detection (LOD) of 0.029 μM, substantially lower than ATPS systems.

Comparative analyses using fluorescence microscopy, microplate readers, and flow cytometry confirmed the superiority of coacervates for isolating and enriching biomolecules, we established that coacervate droplets was approximately 21 times more effective in reducing the LOD for DNA detection compared to ATPS droplets.

This superior performance is largely attributed to non-covalent interactions between DNA and PDDA molecules, involving electrostatic forces and hydrogen bonding. This interaction between biomolecular analytes and coacervate droplets enables ultra-high efficiency in enrichment and thus allows for ultra-sensitive biomolecule quantification without the need for complex instrumentation or signal amplification.

Coacervate-based biosensors, with their enhanced sensitivity and lower detection limits, represent a significant advancement over traditional solid-surface methods like magnetic beads or hydrogels for analyte capture. The liquid nature of coacervates, akin to cellular liquid condensates, better preserves biomolecule structures and simplifies the detection process, reducing the need for additional equipment and laborious washing steps. Our strategy aims to pave the way for simpler, more cost-effective biosensor technologies that can rapidly and accurately detect a wide range of analytes in real-time. The remarkable efficiency of coacervates in biomolecule concentration holds great promise for advancing point-of-care diagnostics, particularly in resource-limited settings, and could be a game-changer in addressing global healthcare challenges.

Experimental section

Materials: Poly(diallyldimethylammonium chloride) (PDDA) with different molecular weights (M_w: < 100 kDa, 100 ~ 200 kDa, 200 ~ 350 kDa, 400 ~ 500 kDa), adenosine 5′-triphosphate disodium salt hydrate (ATP), cytidine 5′-triphosphate disodium salt (CTP), guanosine 5′-triphosphate sodium salt hydrate (GTP), polyethylene glycol (PEG, average M_w = 8000 Da), dextran (M_w = 100 kDa), sodium hydroxide (NaOH, M_w = 40 Da) and Thioflavin T (ThT) were purchased from Sigma-Aldrich. TE buffer (pH 8.0) and sodium phosphate buffer (PBS) were purchased from Sangon Biotech Co., Ltd. (Shanghai, China) and Bibco (Rockville, USA), respectively. Hydrochloric acid (HCl, 36% ~ 38%) was obtained from Guangzhou Donghong Chemical Factory (Guangzhou, China). Oligonucleotide sequences listed in Table 1 were synthesized by Sangon Biotech Co., Ltd. (Shanghai, China).

Table 1. Oligonucleotide sequences used in experiments

Names	Sequences (5' ~ 3')
Cy5-DNA	Cy5-ACGCATCTGTGAAGAGAACCTGGG
Molecular beacon (MB)	FAM-GCGAGCCAGGTTCTCTTCACA GATGCGCTCGC-BHQ1
Target DNA	ACGCATCTGTGAAGAGAACCTGGG
ATP aptamers	ACCTGGGGGAGTATTGCGGAGGAAGGT
Radom sequence R1	TGCAGAGGATGGTTCTGACATCAT
Radom sequence R2	GCTCCATGCTGCGCAGATAATAGC
Radom sequence R3	GAGGAGAAAGCAGTGAGTGGCATA

Methods

Preparation of coacervates and ATPS

PDDA-ATP coacervate samples were obtained by mixing PDDA and ATP solutions in a centrifuge tube. The mixed solution stood for 30 minutes when it got stratified into two aqueous phases. The upper is the dilute phase that contains little PDDA and ATP molecules while the bottom is the condensed coacervate phase. The PDDA-ATP coacervate sample was obtained by removing the upper phase in the tube. To prepare PDDA-ATP coacervate samples with different pH values, 100 μL 5 wt % PDDA (M_w < 100 kDa) solution was mixed with 100 μL 5 wt % ATP solution. The pH of mixed solutions was adjusted by 1 M HCl or 10 M NaOH solution and measured by pH meter (SevenDirect SD50, Mettler Toledo, Switzerland). To prepare PDDA-ATP coacervate samples with different volume ratios of PDDA to ATP solutions (V_P: V_A), 5 wt % PDDA (M_w < 100 kDa) solution was mixed with 5 wt % ATP solution at V_P: V_A = 1:1, 1:2, 1:5, 1:8 and 1:10. To prepare PDDA-ATP coacervate samples with different concentrations of ATP solution, 100 μL 5 wt % PDDA (M_w < 100 kDa) solution was mixed with 100 μL ATP solution. The concentrations of ATP solution were 3 wt %, 5 wt %, 7 wt %, 9 wt % and 11 wt %. To prepare PDDA-ATP coacervate samples with different molecular weights of PDDA, 100 μL 5 wt % PDDA (with M_w < 100 kDa, 100 ~ 200 kDa, 200 ~ 350 kDa, 400 ~ 500 kDa) solution was mixed with 100 μL 5 wt % ATP solution.

To obtain PDDA-ATP aptamer coacervate sample, 100 μL 1 wt % PDDA (with M_w < 100 kDa) solution was mixed with 100 μL ATP aptamer solution (100 μM), which was prepared by dissolving ATP aptamer into TE buffer.

To obtain the two-phase aqueous system (ATPS), 100 μL 16 wt % dextran solution was mixed with 100 μL 20 wt % PEG solution. The pH of the mixed solution was adjusted to 7.

Enrichment of DNA in coacervate under different conditions

To investigate enrichment of DNA in PDDA-ATP coacervates, anthocyanin fluorescent dye (Cy5) was used to label DNA molecules and the fluorescent intensity (FI) of Cy5-DNA in the coacervate could indicate the concentration of DNA enriched in the coacervate ($C_{\mathrm{DNA,\,C}}$). This was achieved by a quantitative relationship between FI and $C_{\mathrm{DNA,\,C}}$ which was established in Figure S1. The diluted concentration of DNA in the bulk solution ($C_{\mathrm{DNA,\,D}}$) was usually too low such that the fluorescence can be hardly detected by the confocal microscope. Therefore, we used the following equation to calculate $C_{\mathrm{DNA,\,D}}$:

$$C_{\mathrm{DNA,\,D}} = \frac{C_{\mathrm{DNA,\,T}}V_{\mathrm{T}} - C_{\mathrm{DNA,\,C}}V_{\mathrm{C}}}{V_{\mathrm{D}}},$$

where V_{T} and $C_{\mathrm{DNA,\,T}}$ are the total volume and concentration of DNA of the sample (containing both the upper bulk and bottom condensed coacervate liquid phases in the tube), respectively, and V_{C} and V_{D} are the volumes of coacervate and bulk liquid phases, respectively. We define an enrichment factor to evaluate the enrichment of DNA in the coacervate by

$$\text{Enrichment Factor} = C_{\mathrm{DNA,\,C}}/C_{\mathrm{DNA,\,D}}.$$

By using this nondimensional parameter, the effects of different conditions on the enrichment of DNA in the coacervate can be illustrated.

To prepare the sample, we added 1 μL of 100 μM Cy5-DNA solution into the 200 μL PDDA/ATP mixed solution. The mixed solution stood for 30 minutes when it got stratified into the upper dilute and bottom condensed liquid phases in the tube. After removing the upper dilute solution, we added 100 μL PBS with the same pH into the tube and completely mixed them. The resulting sample was then observed under Nikon ECLIPSE Ti2 microscope. Each experiment was repeated for three times. Statistic data of fluorescent intensity was obtained and analyzed by Image J.

Target DNA detection

Molecular beacon (MB) is engineered with a fluorophore on one end and a quencher (black hole) on the other, forming a hairpin structure and emitting only a faint fluorescence. In the presence of target DNA, MB, however, unfolds its hairpin structure and hence emits a pronounced fluorescence signal.

The PDDA-ATP coacervate sample was prepared by mixing 100 μL 5 wt % PDDA (M_w < 100 kDa) solution was mixed with 100 μL 5 wt % ATP solution and its pH was adjusted by adding 1 M HCl or 10 M NaOH solution. MB solution was prepared by adding MB into TE buffer. 1 μL 100 μM MB solution was mixed with the coacervate sample in the tube where the target DNA solutions with different concentrations were added and mixed well. After the resulting sample got stratified, the condensed phase was taken for subsequent measurements of fluorescence intensity by the confocal microscope, microplate reader and flow cytometer.

In the Nikon ECLIPSE Ti2 microscope, excitation and emission wavelengths were set to be 460 ~ 550 nm and 520 ~ 530 nm, respectively, and other setting parameters are 200 ms exposure time, and 1.0x live acceleration. In the TECAN Spark multifunction microplate reader, fluorescence intensity was measured with an excitation wavelength of 425 nm and an emission wavelength of 460 ~ 650 nm. Before tested in the Beckman Coulter flow cytometry, the sample was shaken evenly to avoid getting stratified. 20, 000 coacervate droplets were collected using the flow cytometer and the results were visualized by FlowJo.

Target ATP detection

To detect target ATP, PDDA-ATP aptamer coacervate sample containing thioflavin T (ThT) was used. ThT can intercalate into ATP aptamer, enhancing ThT fluorescence. However, when the target ATP is added into the sample, the binding of ATP to its aptamer gives rise to a release of ThT and fluorescence is weakened. 1 μM ThT was added into 100 μL coacervate sample in the tube where the target ATP solutions with different concentrations were added and mixed well. After the resulting solution got stratified, a sample was taken from the bottom of the tube for testing and observation by the confocal microscope.

Determination of limit of detection (LOD)

We evaluated the limit of detection (LOD) from the results obtained by microplate reader in Figure 4b(iii), where fluorescent intensity linearly varied with concentration of target DNA molecules. The slope of the plot is denoted by k. We defined the standard deviation of fluorescent intensity in blank target measurements by σ. LOD is then given by[40]

$$\text{LOD} = \frac{3\sigma}{k}.$$

Calculation of relative optical density

Optical density (OD) of a solution was measured by the microplate reader at 400 nm wavelength. The OD of pure water was $D_0 = 0.0491$. For the coacervate solution (prepared by 0.5 wt %PDDA and 50 μM target DNA), in the absence of any additives such as NaCl and urea, the OD was measured to be $D_1 = 0.217$. At different concentrations of the additives (NaCl or urea), the OD of the coacervate solution was denoted by D_{add}. Then, the relative OD of the additive-laden coacervate solution can be calculated by the equation:

$$\text{Relative OD} = \frac{D_{\text{add}} - D_0}{D_1 - D_0}.$$

Reference

1. Pramesh, C. S.; Badwe, R. A.; Bhoo-Pathy, N.; Booth, C. M.; Chinnaswamy, G.; Dare, A. J.; de Andrade, V. P.; Hunter, D. J.; Gopal, S.; Gospodarowicz, M.; Gunasekera, S.; Ilbawi, A.; Kapambwe, S.; Kingham, P.; Kutluk, T.; Lamichhane, N.; Mutebi, M.; Orem, J.; Parham, G.; Ranganathan, P.; Sengar, M.; Sullivan, R.; Swaminathan, S.; Tannock, I. F.; Tomar, V.; Vanderpuye, V.; Varghese, C.; Weiderpass, E., Priorities for cancer research in low- and middle-income countries: a global perspective. *Nature Medicine* **2022,** *28* (4), 649-657.

2. Kim, J.; Campbell, A. S.; de Ávila, B. E.-F.; Wang, J., Wearable biosensors for healthcare monitoring. *Nature Biotechnology* **2019,** *37* (4), 389-406.

3. Erlich, H. A.; Gelfand, D.; Sninsky, J. J., Recent Advances in the Polymerase Chain Reaction. *Science* **1991,** *252* (5013), 1643-1651.

4. Li; Rothberg, L. J., Label-Free Colorimetric Detection of Specific Sequences in Genomic DNA Amplified by the Polymerase Chain Reaction. *Journal of the American Chemical Society* **2004,** *126* (35), 10958-10961.

5. Yafia, M.; Ymbern, O.; Olanrewaju, A. O.; Parandakh, A.; Sohrabi Kashani, A.; Renault, J.; Jin, Z.; Kim, G.; Ng, A.; Juncker, D., Microfluidic chain reaction of structurally programmed capillary flow events. *Nature* **2022,** *605* (7910), 464-469.

6. Rissin, D. M.; Kan, C. W.; Campbell, T. G.; Howes, S. C.; Fournier, D. R.; Song, L.; Piech, T.; Patel, P. P.; Chang, L.; Rivnak, A. J.; Ferrell, E. P.; Randall, J. D.; Provuncher, G. K.; Walt, D. R.; Duffy, D. C., Single-molecule enzyme-linked immunosorbent assay detects serum proteins at subfemtomolar concentrations. *Nature Biotechnology* **2010,** *28* (6), 595-599.

7. Kim, D.; Kwon, H. J.; Shin, K.; Kim, J.; Yoo, R. E.; Choi, S. H.; Soh, M.; Kang, T.; Han, S. I.; Hyeon, T., Multiplexible Wash-Free Immunoassay Using Colloidal Assemblies of Magnetic and Photoluminescent Nanoparticles. *ACS Nano* **2017,** *11* (8), 8448-8455.

8. Sajali, N.; Wong, S. C.; Hanapi, U. K.; Jamaluddin, S. A. B.; Tasrip, N. A.; Desa, M. N. M., The Challenges of DNA Extraction in Different Assorted Food Matrices: A Review. *J. Food Sci.* **2018,** *83* (10), 2409-2414.

9. Wang, J. H.; Cheng, D. H.; Chen, X. W.; Du, Z.; Fang, Z. L., Direct extraction of double-stranded DNA into ionic liquid 1-butyl-3-methylimidazolium hexafluorophosphate and its quantification. *Anal. Chem.* **2007,** *79* (2), 620-625.

10. Teixeira, A. G.; Agarwal, R.; Ko, K. R.; Grant-Burt, J.; Leung, B. M.; Frampton, J. P., Emerging Biotechnology Applications of Aqueous Two-Phase Systems. *Adv. Healthc. Mater.* **2018,** *7* (6), 19.

11. Albertsson, P. E. R. Å., Partition of Proteins in Liquid Polymer–Polymer Two-Phase Systems. *Nature* **1958,** *182* (4637), 709-711.

12. Ahmed, T.; Yamanishi, C.; Kojima, T.; Takayama, S., Aqueous Two-Phase Systems and Microfluidics for Microscale Assays and Analytical Measurements. *Annual Review of Analytical Chemistry* **2021,** *14* (1), 231-255.

13. Xu, Z.; Wang, S.; Zhao, C.; Li, S.; Liu, X.; Wang, L.; Li, M.; Huang, X.; Mann, S., Photosynthetic hydrogen production by droplet-based microbial micro-reactors under aerobic conditions. *Nature Communications* **2020,** *11* (1), 5985.

14. Chao, Y.; Shum, H. C., Emerging aqueous two-phase systems: from fundamentals of interfaces to biomedical applications. *Chemical Society Reviews* **2020,** *49* (1), 114-142.

15. Qi, C.; Zhou, T.; Wu, X.; Liu, K.; Li, L.; Liu, Z.; Chen, Z.; Xu, J.; Kong, T., Micro-nano-fabrication of green functional materials by multiphase microfluidics for environmental and energy applications. *Green Energy & Environment* **2023**.

16. Cao, Y.; Tian, J. X.; Lin, H. S.; Li, Q. C.; Xiao, Y.; Cui, H. Q.; Shum, H. C., Partitioning-Induced Isolation of Analyte and Analysis via Multiscaled Aqueous Two-Phase System. *Anal. Chem.* **2023,** *95* (10), 4644-4652.

17. Minagawa, Y.; Nakata, S.; Date, M.; Ii, Y.; Noji, H., On-Chip Enrichment System for Digital Bioassay Based on Aqueous Two-Phase System. *ACS Nano* **2023,** *17* (1), 212-220.

18. Li, Z.; McNeely, M.; Sandford, E.; Tewari, M.; Johnson-Buck, A.; Walter, N. G., Attomolar Sensitivity in Single Biomarker Counting upon Aqueous Two-Phase Surface Enrichment. *ACS Sens.* **2022,** *7* (5), 1419-1430.

19. Chen, Q.; Zhang, Y.; Chen, H.; Liu, J.; Liu, J., Enhancing the Sensitivity of DNA and Aptamer Probes in the Dextran/PEG Aqueous Two-Phase System. *Analytical Chemistry* **2021,** *93* (24), 8577-8584.

20. Liu, Z.; Zhou, W.; Qi, C.; Kong, T., Interface Engineering in Multiphase Systems toward Synthetic Cells and Organelles: From Soft Matter Fundamentals to Biomedical Applications. *Advancd Materials* **2020,** *32*, 2002932.

21. Guindani, C.; da Silva, L. C.; Cao, S.; Ivanov, T.; Landfester, K., Synthetic Cells: From Simple Bio-Inspired Modules to Sophisticated Integrated Systems. *Angewandte Chemie International Edition* **2022,** *61* (16), e202110855.

22. Brangwynne, C. P.; Eckmann, C. R.; Courson, D. S.; Rybarska, A.; Hoege, C.; Gharakhani, J.; Jülicher, F.; Hyman, A. A., Germline P Granules Are Liquid Droplets That Localize by Controlled Dissolution/Condensation. *Science* **2009,** *324* (5935), 1729-1732.

23. Wippich, F.; Bodenmiller, B.; Trajkovska, Maria G.; Wanka, S.; Aebersold, R.; Pelkmans, L., Dual Specificity Kinase DYRK3 Couples Stress Granule Condensation/Dissolution to mTORC1 Signaling. *Cell* **2013,** *152* (4), 791-805.

24. Li, P.; Banjade, S.; Cheng, H.-C.; Kim, S.; Chen, B.; Guo, L.; Llaguno, M.; Hollingsworth, J. V.; King, D. S.; Banani, S. F.; Russo, P. S.; Jiang, Q.-X.; Nixon, B. T.; Rosen, M. K., Phase transitions in the assembly of multivalent signalling proteins. *Nature* **2012,** *483* (7389), 336-340.

25. Li, Q.; Song, Q.; Guo, W.; Cao, Y.; Cui, X.; Chen, D.; Shum, H. C., Synthetic Membraneless Droplets for Synaptic-Like Clustering of Lipid Vesicles. *Angewandte Chemie International Edition* **2023,** *62* (45), e202313096.

26. Xu, C.; Martin, N.; Li, M.; Mann, S., Living material assembly of bacteriogenic protocells. *Nature* **2022,** *609* (7929), 1029-1037.

27. Garenne, D.; Beven, L.; Navailles, L.; Nallet, F.; Dufourc, E. J.; Douliez, J.-P., Sequestration of Proteins by Fatty Acid Coacervates for Their Encapsulation within Vesicles. *Angewandte Chemie International Edition* **2016,** *55* (43), 13475-13479.

28. Agrawal, A.; Douglas, J. F.; Tirrell, M.; Karim, A., Manipulation of coacervate droplets with an electric field. *Proceedings of the National Academy of Sciences* **2022,** *119* (32), e2203483119.

29. Lu, T.; Spruijt, E., Multiphase Complex Coacervate Droplets. *Journal of the American Chemical Society* **2020,** *142* (6), 2905-2914.

30. Shin, Y.; Brangwynne, C. P., Liquid phase condensation in cell physiology and disease. *Science* **2017,** *357* (6357), eaaf4382.

31. Gouveia, B.; Kim, Y.; Shaevitz, J. W.; Petry, S.; Stone, H. A.; Brangwynne, C. P., Capillary forces generated by biomolecular condensates. *Nature* **2022,** *609* (7926), 255-264.

32. Zhang, S.; Qi, C.; Zhang, W.; Zhou, H.; Wu, N.; Yang, M.; Meng, S.; Liu, Z.; Kong, T., In Situ Endothelialization of Free-Form 3D Network of Interconnected Tubular Channels via Interfacial Coacervation by Aqueous-in-Aqueous Embedded Bioprinting. *Advanced Materials* **2023,** *35* (7), 2209263.

33. Guo, W.; Kinghorn, A. B.; Zhang, Y.; Li, Q.; Poonam, A. D.; Tanner, J. A.; Shum, H. C., Non-associative phase separation in an evaporating droplet as a model for prebiotic compartmentalization. *Nature Communications* **2021,** *12* (1), 3194.

34. Nazer, B.; Dehghani, M. R.; Goliaei, B., Plasmid DNA affinity partitioning using polyethylene glycol – sodium sulfate aqueous two-phase systems. *Journal of Chromatography B* **2017,** *1044-1045*, 112-119.

35. Liu, S.; Zhang, Y.; He, X.; Li, M.; Huang, J.; Yang, X.; Wang, K.; Mann, S.; Liu, J., Signal processing and generation of bioactive nitric oxide in a model prototissue. *Nature Communications* **2022,** *13* (1), 5254.

36. Chen, Y.; Yuan, M.; Zhang, Y.; Liu, S.; Yang, X.; Wang, K.; Liu, J., Construction of coacervate-in-coacervate multi-compartment protocells for spatial organization of enzymatic reactions. *Chemical Science* **2020,** *11* (32), 8617-8625.

37. Shang, L.; Ye, F.; Li, M.; Zhao, Y., Spatial confinement toward creating artificial living systems. *Chemical Society Reviews* **2022,** *51* (10), 4075-4093.

38. Zhang, Y.; Wang, Z.; Li, M.; Xu, C.; Gao, N.; Yin, Z.; Wang, K.; Mann, S.; Liu, J., Osmotic-Induced Reconfiguration and Activation in Membranized Coacervate-Based Protocells. *Journal of the American Chemical Society* **2023,** *145* (18), 10396-10403.

39. Poudyal, M.; Patel, K.; Gadhe, L.; Sawner, A. S.; Kadu, P.; Datta, D.; Mukherjee, S.; Ray, S.; Navalkar, A.; Maiti, S.; Chatterjee, D.; Devi, J.; Bera, R.; Gahlot, N.; Joseph, J.; Padinhateeri, R.; Maji, S. K., Intermolecular interactions underlie protein/peptide phase separation irrespective of sequence and structure at crowded milieu. *Nature Communications* **2023,** *14* (1), 6199.

40. Liu, H.-C.; Ruan, K.; Ma, K.; Fei, J.; Lin, Y.-M.; Xia, H., Synthesis of metalla-dual-azulenes with fluoride ion recognition properties. *Nature Communications* **2023,** *14* (1), 5583.

Author Contributions

C. Qi, and T. T. Kong conceived, designed, and supervised the project. C. Cen, X. Ma, and X. Lu performed experiments. H. Zhou, S. Meng, Z. Liu, W. Chen, C. Qi, and T. T. Kong analyzed the data. C. Qi and T. T. Kong wrote the manuscript. The manuscript was written through contributions of all authors. All authors have given approval to the final version of the manuscript.

Notes

The authors declare no competing financial interest.

Acknowledgements

The authors thank Dr. Chengbing Yang for his helpful suggestions and discussions. This work was supported by National Natural Science Foundation of China (Grant Nos. 22078197, 52172283, 22308219), Guangdong Basic and Applied Basic Research

Foundation (Grant Nos. 2021A1515012506, 2023A1515011827), Shenzhen Science and Technology Program (JCYJ20220818095801003, RCYX20221008092902010) and Shenzhen Natural Science Fund (the Stable Support Plan Program 20220810120421001).